

UKAEA-CCFE-CP(19)39

F. Riva, F. Militello, J. T. Omotani, B. Dudson, S. D. Elmore, S. Newton, T. Nicholas, N. R. Walkden, the MAST team

Comparison of three-dimensional plasma edge turbulence simulations in realistic double null tokamak geometry with experimental observations

This document is intended for publication in the open literature. It is made available on the understanding that it may not be further circulated and extracts or references may not be published prior to publication of the original when applicable, or without the consent of the UKAEA Publications Officer, Culham Science Centre, Building K1/0/83, Abingdon, Oxfordshire, OX14 3DB, UK.

Enquiries about copyright and reproduction should in the first instance be addressed to the UKAEA Publications Officer, Culham Science Centre, Building K1/0/83 Abingdon, Oxfordshire, OX14 3DB, UK. The United Kingdom Atomic Energy Authority is the copyright holder.

The contents of this document and all other UKAEA Preprints, Reports and Conference Papers are available to view online free at <https://scientific-publications.ukaea.uk/>

Comparison of three-dimensional plasma edge turbulence simulations in realistic double null tokamak geometry with experimental observations

F. Riva, F. Militello, J. T. Omotani, B. Dudson, S. D. Elmore, S. Newton, T. Nicholas, N. R. Walkden, the MAST team

Three-dimensional plasma edge turbulence simulations of MAST and comparison with experimental measurements

F. Riva¹, F. Militello¹, J. T. Omotani¹, B. Dudson², S. D. Elmore¹, S. Newton¹, T.

Nicholas^{1,2}, N. R. Walkden¹ and the MAST team

¹*United Kingdom Atomic Energy Authority, Culham Centre for Fusion Energy, Culham Science Centre, Abingdon, Oxon, OX14 3DB, UK*

²*York Plasma Institute, Department of Physics, University of York, Heslington, York YO10 5DQ, UK*

In this work we report on the comparison between a disconnected double null MAST plasma discharge and the first three-dimensional fluid turbulence simulations carried out with the STORM module [1] of BOUT++ [2] in such geometry. Specifically, we carried out a number of simulations with STORM focusing on the ohmic deuterium L-mode pulse #21712 and we compare the results with experimental observations.

Due to the high plasma collisionality typical of the tokamak scrape-off layer (SOL) in L-mode, medium-size devices, the STORM model is based on a set of electrostatic drift-reduced Braginskii equations. Additionally, the cold-ion and Boussinesq approximations are employed to simplify the equations, and plasma-neutral interactions are neglected. The resulting system of equations corresponds to an extension of the one used in Ref. [1] with the inclusion of metric terms accounting for the realistic three-dimensional axisymmetric magnetic geometry. The STORM model used for the present investigation therefore includes: (i) a continuity equation, ensuring conservation of plasma density; (ii) a vorticity equation, used to impose charge conservation; (iii) electron and ion parallel momentum equations; and (iv) an energy equation for electrons. The system is closed by the Poisson equation $\nabla \cdot (\nabla_{\perp} \phi / B^2) = \Omega$, with ϕ the electrostatic potential and Ω the plasma vorticity, and completed by a set of boundary conditions describing the plasma dynamics at the magnetic pre-sheath entrance.

A field-aligned coordinate system is employed to express the STORM model equations. All radial and parallel derivatives are computed using second order centered finite difference schemes, except for the ExB advection operator, discretized with a second order Arakawa scheme, and the parallel advection terms, discretized with second order upwind schemes. Additionally, we exploit periodicity in the toroidal angle to perform toroidal derivatives in Fourier space. Time integration is performed adopting the Method of Lines approach. Grid-scale oscillations are avoided by staggering the flux variables half a point in the parallel direction.

Four simulations are carried out, with (i) reference collisional parameters for the plasma discharge #21712 (“Reference” simulation) (ii) increased normalized resistivity by a factor 5 (“High η_{\parallel} ” simulation); (iii) increased viscosity by a factor 6 (“High $\mu_{\Omega 0}$ ” simulation); and (iv) perpendicular dissipation parameters decreased by a factor 4 (“Low \perp dissipation” simulation). The simulations are initialized from ad hoc axisymmetric profiles, to which small amplitude random noise is added. Axisymmetric density and energy sources located at and inside the last closed flux surface (LCFS) then inject plasma particles and heat, steepening the plasma profiles and triggering plasma-gradient driven instabilities. After an initial transient phase, a statistical steady state is reached, in which the sources are balanced by the parallel losses at the divertor plates and by the turbulent radial transport. In the following, we focus our analysis only on this saturated statistical steady state. We note that the grid chosen for our simulations ensures a perpendicular resolution at the mid-planes up to $k_{\perp}\rho_{s0} \simeq 1$, with $\rho_{s0} \approx 2$ mm.

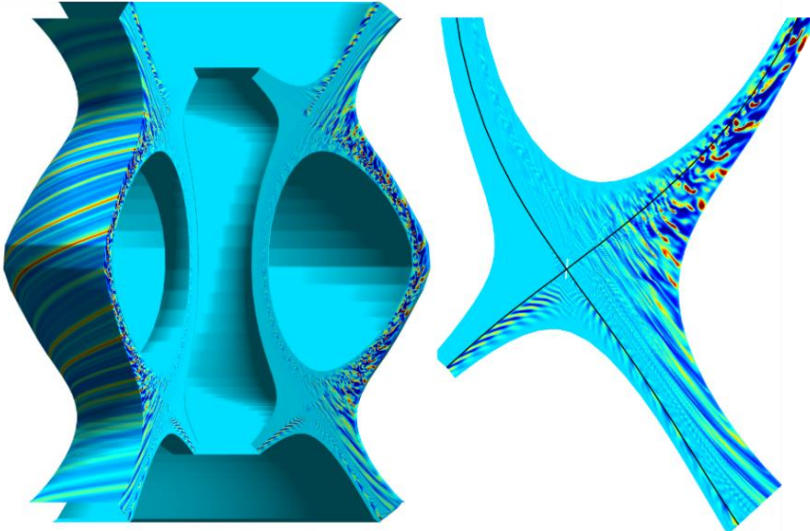


Figure 1: (left) Relative plasma density perturbations. (right) Zoom on the lower X-point region. The black line denotes the inner separatrix.

An example of a snapshot obtained from a STORM simulation is shown in Fig. 1, left. We observe that plasma turbulence develops inside the last closed flux surface, with fluctuations having a ballooning character. Because of the strong magnetic shear near the X-points, filaments are more homogenous along

magnetic field lines in the far SOL than near the separatrix (see Fig. 1, right). The numerical results are in qualitative agreement with previous experimental observations, with filaments showing different properties in the main SOL, in the private flux regions and in divertor legs [3]. Additionally, striations on the divertor plates, as are seen with infrared imaging diagnostics [4], are also reproduced by our simulations (not shown here).

To perform a more quantitative comparison of STORM simulations with experimental measurements, we post-process the simulation results with a synthetic reciprocating probe and we compare the results with measurements from a Gundestrup probe that was installed on a reciprocating manipulator at the outer mid-plane of MAST. In Fig. 2 we display the time-averaged ion saturation current, I_{sat} , and floating potential, V_{fl} , profiles [(a) and (b)], for the

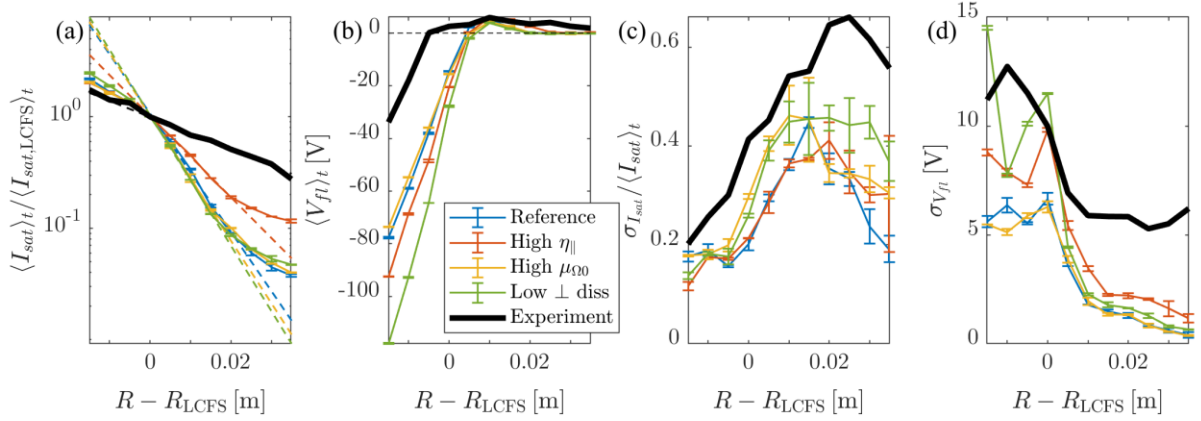


Figure 2: I_{sat} and V_{fl} time-averaged [(a) and (b)] and fluctuation [(c) and (d)] profiles for the experimental measurements (thick black lines) and the STORM simulations (thin color lines). The dashed lines in (a) denote an exponential best-fit.

experimental measurements (thick black lines) and the four simulations discussed above (thin color lines), with the I_{sat} profiles normalized to their values at the LCFS. The time-averaged I_{sat} profiles are steeper in the simulations than in the experiment, in particular in the proximity of the LCFS. Furthermore, the perpendicular collisional dissipation parameters seem to play a minor role in setting I_{sat} gradient scale lengths, whereas the Spitzer resistivity has a stronger impact. We also best-fit the profiles shown in Fig. 2 (a) with an exponential (dashed lines), finding that the I_{sat} gradient scale lengths are approximately 4 times smaller in the numerical results than in the experiment. Concerning the V_{fl} time-averaged profiles, we see that numerical results and experimental measurements are in qualitative agreement, increasing in the core and decreasing in the SOL. However, the experimental profile in the core is radially shifted with respect to the numerical results.

In Fig. 2 we also display the amplitude of normalized I_{sat} and V_{fl} fluctuations [(c) and (d)] for the experiment and the simulations. The trends in the experiment are well captured by the simulations, with relative I_{sat} fluctuations increasing and V_{fl} fluctuations decreasing as we move radially outwards. Despite the good qualitative agreement, Figs. 2 (c) and (d) show that the simulations underestimate the amplitude of the fluctuations.

To investigate if these discrepancies are related to differences between the experiment and the simulations in some particular properties of plasma turbulence, we compared several additional statistical properties of I_{sat} and V_{fl} time traces, including the skewness and the kurtosis of the probability distribution functions (PDFs) as function of the radial position, and the PDFs and power spectral densities at different radial locations; as well as some statistical properties of intermittent events, including I_{sat} and V_{fl} conditional averaged temporal wave forms, auto-correlation functions of I_{sat} and V_{fl} fluctuations, average time spent by I_{sat} and V_{fl} signals above and below a given threshold, and averaged waiting time between I_{sat} and V_{fl} maxima. Overall,

in the SOL we find good qualitative and quantitative agreement between simulations and experiment.

To conclude our discussion, we note that some preliminary analysis of an additional simulation performed without the Boussinesq approximation suggests that time-averaged I_{sat} profiles are steeper in the simulations than in the experiment because of higher parallel losses. In particular, the electron parallel currents flowing to the divertor targets near the separatrix are three to four times larger with the Boussinesq approximation implemented in STORM than without it. A more detailed investigation of these results will be performed in the future to elucidate how the Boussinesq approximation affects the properties of SOL plasma turbulence.

In summary, in the present work we display the first global flux-driven STORM simulations based on the MAST L-mode plasma discharge #21712 in double null configuration. This represents a major step in the development of STORM, which is now able to simulate plasma turbulence at the edge of tokamak devices such as MAST in realistic diverted configurations. The simulations are then compared with experimental measurements, finding good qualitative agreement. However, the time-averaged profiles at the outer mid-plane are steeper in the simulations than in the experiment, resulting in an ion saturation current decay length approximately 4 times smaller in the numerical results than in the experimental measurements. The impact of the Boussinesq approximation on the I_{sat} decay length is also investigated, showing how it may affect the simulation results.

This work has been carried out within the framework of the EUROfusion Consortium and has received funding from the Euratom research and training programme 2014-2018 and 2019-2020 under grant agreement No 633053 and from the RCUK [grant number EP/P012450/1]. The views and opinions expressed herein do not necessarily reflect those of the European Commission.

[1] N. R. Walkden *et al.*, Plasma Phys. Control. Fusion **58**, 115010 (2016)

[2] B. D. Dudson *et al.*, Comput. Phys. Commun. **180**, 1467–1480 (2009)

[3] J. Harrison *et al.*, Phys. Plasmas **22**, 092508 (2015)

[4] R. J. Maqueda *et al.*, Nucl. Fusion **50**, 075002 (2010)